

Ground-state stability and excitation spectrum of a one-dimensional dipolar supersolid

Tobias Ilg¹ and Hans Peter Büchler¹

¹*Institute for Theoretical Physics III and Center for Integrated Quantum Science and Technology,
University of Stuttgart, DE-70550 Stuttgart, Germany*

(Dated: December 1, 2022)

We study the behavior of the excitation spectrum across the quantum phase transition from a superfluid to a supersolid phase of a dipolar Bose gas confined to a one-dimensional geometry. Including the leading beyond-mean-field effects within an effective Hamiltonian, the analysis is based on Bogoliubov theory with several order parameters accounting for the superfluid as well as solid structure. We find fast convergence of the ground-state energy in the supersolid with the number of order parameters and demonstrate a stable excitation spectrum with two Goldstone modes and an amplitude mode in the low-energy regime. Our results imply that for realistic experimental parameters with Dysprosium atoms, the supersolid phase is stable in the thermodynamic limit and the transition into the supersolid phase is of second order driven by the roton instability.

I. INTRODUCTION

Breakthrough experiments with weakly interacting dipolar Bose gases have recently demonstrated the appearance of a supersolid phase in elongated traps [1–3]. The phase transition is accompanied by the appearance of a roton minimum in the excitation spectrum [4, 5]. Remarkably, the description within the Gross-Pitaevskii formalism requires the inclusion of the leading beyond-mean-field correction for the stability of the droplets [6, 7]. Such numerical studies within the experimental three-dimensional setting are in good agreement with experimental observations in dipolar quantum gases [8, 9]. In this manuscript, we study whether this supersolid phase is stable in the thermodynamic limit and derive the low-energy excitation spectrum across the phase transition from the superfluid to the supersolid phase within Bogoliubov theory.

The possibility of a ground state for interacting bosonic particles which combines the density modulation of a solid and the frictionless flow of a superfluid has been shown by A. J. Leggett [10]. Especially solid helium has been discussed as a candidate for this exotic state of matter, a system with nearly one atom per unit cell [11–13]. In contrast, the current experiments with Dysprosium atoms work in a rather complementary regime and realize a supersolid state with several thousand atoms on each lattice site; a parameter regime, where one can expect mean-field theory to describe the supersolid phase accurately. The main ingredient for the appearance of the supersolid state is the combination of a tunable short-range interaction with a magnetic dipole-dipole interaction. For increasing influence of the dipolar interaction, such systems can undergo an instability towards the formation of quantum droplets [6, 14–23], as well as self-bound droplets [19, 24–28], or supersolid states [1–3, 29–54]. An important observation was that these states are only stabilized by the leading beyond-mean-field correction, which provides an additional contribution to the energy functional stabilizing the system at higher densities against a collapse [6]; such a stabilization has pre-

viously been predicted for Bose mixtures [7] and later also experimentally observed [55]. Within local-density approximation, this additional term can be included into the Gross-Pitaevskii functional and forms the basis for extensive numerical studies of the supersolid state and its excitation spectrum. However, the nature of the transition is often difficult to access in such fully numerical approaches in a finite size setting [38].

Here, we present an analytical study on the nature of the quantum phase transition from a superfluid to the supersolid in the thermodynamic limit and analyze the excitation spectrum across the transition. The analysis is based on Bogoliubov theory in a one-dimensional setting, where we account for the transverse confinement by a variational ansatz and include the beyond-mean-field contributions within an effective Hamiltonian. The supersolid state is described by the macroscopic occupation of additional modes giving rise to additional order parameters. We demonstrate that the ground-state energy close to the quantum phase transition converges very quickly for increasing number of order parameters, and demonstrate that the excitation spectrum is stable. Especially, we find in the low-energy regime two gapless modes in agreement with the two broken continuous symmetries as well as a gapped amplitude mode for the solid structure. For parameters comparable to current experiments with Dysprosium atoms, this analysis confirms that the beyond-mean-field corrections stabilize the supersolid phase within a one-dimensional geometry and demonstrates that the phase transition within mean-field theory can be of second order and driven by the roton instability, depending on exact system parameters.

The manuscript is structured as follows. In Sec. II we discuss the treatment of the superfluid phase in the one-dimensional geometry and how to include quantum fluctuations in our approach. Within our model, we discuss excitations in the superfluid in Sec. III and briefly examine the roton instability in Sec. IV. Then, we adapt our approach in Sec. V to describe the one-dimensional supersolid and calculate its excitation spectrum in Sec. VI. Lastly, we summarize our results in Sec. VII.

II. SUPERFLUID PHASE

In this manuscript, we calculate the excitation spectrum across the phase transition from a Bose-Einstein condensate into the supersolid regime within a simple reduced three-dimensional model [43] using Bogoliubov theory and include beyond-mean-field corrections in local-density approximation. We consider a gas of trapped dipolar Bosons with mass m , which are tightly confined in the x - y plane by a harmonic confinement but free along the z -direction. The validity of the local-density approximation requires that the characteristic healing length ξ of the superfluid is smaller than the harmonic oscillator length l_\perp of the transverse confinement, i.e., $\xi/l_\perp \ll 1$, see Ref. [56]. In the following, we are interested in the low-energy excitations and the stability analysis of the supersolid phase. For these considerations, transverse excitations can be ignored and we make a variational ansatz for the transverse wave function, $\psi(x, y) = \exp[-(\nu x^2 + y^2/\nu)/2(\sigma l_\perp)^2]/(\sqrt{\pi}\sigma l_\perp)$, with the dimensionless variational parameters σ and ν determined by minimizing the ground-state energy (see below). Within this variational framework, the microscopic Hamiltonian becomes one-dimensional and consists of two parts, $H_0 + H_1$. The single-particle Hamiltonian is described by $H_0 = \sum_q [\epsilon_0(q) + E_t(\sigma, \nu)] a_q^\dagger a_q$, where a_q^\dagger (a_q) are the bosonic creation (annihilation) operators of particles with momentum q , respectively. The first term accounts for the kinetic energy along the tube with the dispersion relation $\epsilon_0(q) = \frac{\hbar^2 q^2}{2m}$, while $E_t(\sigma, \nu) = E_\perp(\frac{1}{\nu} + \nu)(\frac{1}{\sigma^2} + \sigma^2)/4$ accounts for the energy of the particles in the transverse trap with $E_\perp = \hbar^2/m l_\perp^2$. The particles interact via a short-range contact interaction characterized by the s -wave scattering length a_s and the anisotropic magnetic dipole-dipole interaction with strength a_{dd} . The dipoles are aligned perpendicular to the z -direction. By integrating out the transverse degrees of freedom using the variational wave function, the two-body potential in momentum space is well described by [57]

$$V(q) = g_{\text{1D}} \left[1 + \varepsilon_{\text{dd}} \left(\frac{3(1 - Qe^Q \Gamma(0, Q))}{1 + \nu} - 1 \right) \right],$$

with $g_{\text{1D}} = 2\hbar^2 a_s/(m\sigma^2 l_\perp^2)$, $Q = \sqrt{\nu}(q\sigma l_\perp)^2/2$ and $\varepsilon_{\text{dd}} = a_{\text{dd}}/a_s$. Here, $\Gamma(s, x)$ denotes the incomplete Gamma function. Corrections of g_{1D} due to the confinement-induced resonance are only relevant for $\xi/l_\perp \gg 1$ [56, 58], and therefore can be ignored here. Then, the interaction part of the Hamiltonian is given by

$$H_1 = \frac{1}{2L} \sum_{p, k, q} V(q) a_{p+q}^\dagger a_{k-q}^\dagger a_k a_p,$$

where L is the quantization volume. From the microscopic Hamiltonian one obtains the mean-field energy the single-particle Bogoliubov excitation spectrum as well as the leading beyond-mean-field correction within standard

Bogoliubov theory. However, it is well established that for dipolar quantum gases, the beyond-mean-field correction plays a crucial role in stabilizing the quantum droplets and needs to be included when describing the excitation spectrum. So far, the analysis is mainly based on numerical studies of the extended Gross-Pitaevskii equation, where the beyond mean-field term is included within local-density approximation [38]. In analogy, we add a term H_{LHY} to the Hamiltonian such that Bogoliubov theory on this effective Hamiltonian properly accounts for the low-energy excitations within Bogoliubov theory; this method is equivalent to studying the excitation spectrum within the extended Gross-Pitaevskii equation, but more suitable for our analytical study.

The beyond-mean-field correction for a three-dimensional dipolar Bose-Einstein condensate has been determined in Ref. [59, 60]. The energy density takes the form

$$u_{\text{LHY}} = \frac{256\sqrt{\pi}\hbar^2}{15m} (n_{\text{3D}} a_s)^{5/2} Q_5(\varepsilon_{\text{dd}}),$$

with $Q_5(\varepsilon_{\text{dd}}) = \int_0^1 du (1 - \varepsilon_{\text{dd}} + 3\varepsilon_{\text{dd}} u^2)^{5/2}$ and n_{3D} the density of the homogeneous three-dimensional system. The function $Q_5(\varepsilon_{\text{dd}})$ accounts for the modification due to the additional dipolar interaction to the well established result for contact interactions derived by Lee, Huang and Yang (LHY) [61, 62]. Within this derivation, one finds that the LHY correction is dominated by excitations around the momenta $1/\xi$ with characteristic length scale $\xi = \hbar/\sqrt{2mn_{\text{3D}}g}$. This implies that the local-density approximation is well justified, if the density varies smoothly on this characteristic scale ξ , i.e., $l_\perp \gg \xi$. Within local-density approximation and the using the variational wave function $\psi(x, y)$, we end up with the correction

$$\frac{E_{\text{LHY}}}{L} = \frac{2}{5} \gamma n^{5/2} \quad \text{where} \quad \gamma = \frac{256}{15\pi} \frac{\hbar^2}{m(\sigma l_\perp)^3} Q_5(\varepsilon_{\text{dd}}) a_s^{5/2}.$$

The ground-state energy including the LHY correction hence becomes

$$\frac{E}{L} = \min_{\sigma, \nu} \left[n E_t(\sigma, \nu) + \frac{1}{2} n^2 V(0) + \frac{2}{5} \gamma n^{5/2} \right],$$

with n the one-dimensional particle density $n = N/L$. The correction to the mean-field energy provides a correction in the chemical potential

$$\mu = \frac{dE}{dN} = E_t + nV(0) + \gamma n^{3/2}, \quad (1)$$

where N is the particle number. Note, that σ and ν are only very weakly depending on the number of particles and within our analysis we self-consistently ignore this small contribution. Accordingly, a correction to the chemical potential affects the compressibility $\varkappa = d\mu/dn$, which gives rise to a modified sound velocity of the superfluid,

$$c^2 = \frac{n\varkappa}{m} = \frac{1}{m} \left(nV(0) + \frac{3}{2} \gamma n^{3/2} \right).$$

The term H_{LHY} we add to the Hamiltonian is therefore determined such that it reproduces the correct ground-state energy E within mean-field as well as the correct sound velocity as the low-momentum limit of the excitation spectrum $\epsilon(q)$ within lowest order Bogoliubov theory. The contribution to the Hamiltonian, which fulfills these conditions can be written as

$$H_{\text{LHY}} = \frac{2}{5}\gamma \int dz (\Psi^\dagger(z)\Psi^\dagger(z)\Psi(z)\Psi(z))^{5/4}$$

with

$$\Psi(z) = \frac{1}{\sqrt{L}} \sum_q e^{iqz} a_q,$$

as will be demonstrated below. The effective Hamiltonian

$$H = H_0 + H_I + H_{\text{LHY}} \quad (2)$$

will allow us to determine the low-energy excitation spectrum across the phase transition from the superfluid to the supersolid. The validity of our approach is limited to momentum $q \ll 1/\xi$ and energies $\epsilon(q) \ll \mu$ such that the local-density treatment for the term H_{LHY} is justified. In addition we require $\epsilon(q) \lesssim E_\perp$ in order to neglect transverse excitations.

III. EXCITATIONS IN THE SUPERFLUID PHASE

We start with the study of the excitation spectrum in the superfluid using the standard Bogoliubov procedure [63]. It is important to point out, that even in one dimension, the Bogoliubov theory provides the correct excitation spectrum in the weakly interacting regime as can be seen by a comparison with the exact Lieb-Liniger theory for Bosons with contact interactions [64, 65]. One can understand this phenomenon as locally there is still a high number of particles in the condensate, while quantum fluctuations only suppress the coherence between these local condensates on large distances giving rise to the well established algebraic behavior [66, 67]. In the following, it is convenient to work in the grand canonical ensemble described by the chemical potential μ and self-consistently determine the chemical potential to find the correct particle density n . Within mean-field theory, we replace the operator $a_0^\dagger = \sqrt{Ln}$ by the local particle density. Inserting this ansatz in the grand canonical potential Ω provides, as required, the ground-state energy including the LHY correction,

$$\Omega = E - \mu N,$$

and we recover the relation between the particle number n and the chemical potential in Eq. (1) by minimizing Ω . In the next step, we can use the standard Bogoliubov

prescription to derive the excitation spectrum. For this purpose, we write for the bosonic field operator

$$\Psi(z) \rightarrow \sqrt{n} + \frac{1}{\sqrt{L}} \sum_{q \neq 0} e^{iqz} a_q = \sqrt{n} + \delta\psi(z).$$

Note, that within this approach with fixed chemical potential and leading order expansion, we do not have to distinguish between the particle density n and the condensate density n_0 , as the difference only becomes relevant for the higher order corrections. Inserting the bosonic field operator into the Hamiltonian and expanding it up to second order in the small fluctuations $\delta\psi$, we end up with a quadratic Hamiltonian H_{B} accounting for the Bogoliubov excitations

$$H_{\text{B}} = \frac{1}{2} \sum_{q \neq 0} : \begin{pmatrix} a_q^\dagger \\ a_{-q} \end{pmatrix} \left[\begin{pmatrix} \chi & 0 \\ 0 & \chi \end{pmatrix} + \begin{pmatrix} \eta & \eta \\ \eta & \eta \end{pmatrix} \right] \begin{pmatrix} a_q \\ a_{-q}^\dagger \end{pmatrix} : . \quad (3)$$

Here, $:\hat{O}:$ denotes the normal ordered operator \hat{O} , and we introduced the two parameters

$$\begin{aligned} \chi &= \epsilon_0(q) + E_t + nV(0) + \gamma n^{3/2} - \mu, \\ \eta &= nV(q) + \frac{3}{2}\gamma n^{3/2}. \end{aligned}$$

To obtain the excitation spectrum $\epsilon(q)$, we diagonalize the Hamiltonian (3) via the Bogoliubov transformation $a_q = u_q b_q + v_q b_{-q}^\dagger$. The amplitudes u_p and v_p have to fulfill the constraint $u_p^2 - v_p^2 = 1$ for the transformation to be canonical. A short calculation yields the diagonal Hamiltonian for the excitation spectrum

$$H_{\text{B}} = \sum_{q \neq 0} \epsilon(q) b_q^\dagger b_q,$$

where the Bogoliubov excitation spectrum is given by

$$\epsilon(q)^2 = \chi^2 + 2\chi\eta. \quad (4)$$

The Bogoliubov excitation spectrum $\epsilon(q)$ depends on the chemical potential. However, using the correct chemical potential in Eq. (1) including the LHY correction, the excitation spectrum becomes gapless,

$$\epsilon(q)^2 = \epsilon_0(q)^2 + 2\epsilon_0(q) \left[nV(q) + \frac{3}{2}\gamma n^{3/2} \right], \quad (5)$$

as required by the famous Hugenholtz and Pines relation [68]. At low momenta, we recover the predicted sound velocity,

$$\epsilon(q) \stackrel{q \rightarrow 0}{=} \hbar |q| c,$$

with c given in Eq. (2). Therefore, we demonstrated that our effective approach with the Hamiltonian in Eq. (2) is capable to reproduce the low-energy excitation spectrum within Bogoliubov theory.

IV. ROTON INSTABILITY

The competition of the contact repulsion between the bosons and the attractive part of the dipole-dipole interaction provides a characteristic Bogoliubov excitation spectrum exhibiting a roton-like structure in the tube. Especially, for an increasing strength of the dipole-dipole interaction, the excitation spectrum exhibits a minimum at a finite momentum k_{\min} , which eventually can reach zero and gives rise to an instability of the superfluid. We will briefly discuss the behavior of the excitation spectrum. The two different interactions in combination with the transverse trapping potential offer a high level of control on the spectrum. The different parameters are most conveniently expressed by the dimensionless quantities

$$\kappa = na_s \propto \frac{l_{\perp}^2}{\xi^2}, \quad \varepsilon_{\text{dd}} = \frac{a_{\text{dd}}}{a_s} \quad \text{and} \quad \lambda = \frac{a_s}{l_{\perp}}.$$

Here, κ controls the dimensionality of the system, and in our one-dimensional geometry within local-density approximation we require $\kappa \gg 1$. In addition, the condition of a weakly interacting Bose gas requires $\lambda \ll 1$ [56]. By tuning these three parameters, the position and energy of the roton excitation can be influenced. We are interested in the region, where the superfluid becomes unstable and transitions to the supersolid phase. This critical point is determined by the two conditions,

$$\epsilon(k_{\text{r}})^2 = 0, \quad \text{and} \quad \left. \frac{d\epsilon(q)^2}{dq} \right|_{q=k_{\text{r}}} = 0,$$

which we solve numerically. For our discussion, we consider a parameter regime comparable to recent Dysprosium experiments [2, 29]. Throughout this manuscript we set the instability to appear at $\kappa_{\text{c}} = 11.931$ and $\lambda_{\text{c}} = 1/200$, which provides the critical values $\varepsilon_{\text{dd},\text{c}} = 1.34$, $k_{\text{r}}l_{\perp} = 1.570$ and allows for a second-order phase transition (see below). Note, that the wave vector k_{r} of the roton instability for these parameters satisfies the condition of low momenta with $k_{\text{r}} < 1/\xi$. It should also be noted, that for $\varepsilon_{\text{dd}} > 1$ the function $\mathcal{Q}_5(\varepsilon_{\text{dd}})$ picks up a very small imaginary part. This contribution is an unphysical artifact from local-density approximation since a three-dimensional homogeneous dipolar gas exhibits a phonon instability for $\varepsilon_{\text{dd}} > 1$ [69]. Therefore we drop the imaginary part in the following. In Fig. 1 we compare the excitation spectrum from Eq.(5) for different values of ε_{dd} . We want to point out that changing ε_{dd} experimentally is achieved by tuning the scattering length a_s which also affects κ and λ . By increasing ε_{dd} a minimum develops, which eventually reaches zero energy at the critical point $\varepsilon_{\text{dd},\text{c}}$. For $\varepsilon_{\text{dd}} > \varepsilon_{\text{dd},\text{c}}$ the excitation spectrum becomes imaginary close to the roton momentum indicating an instability and a breakdown of our current treatment.

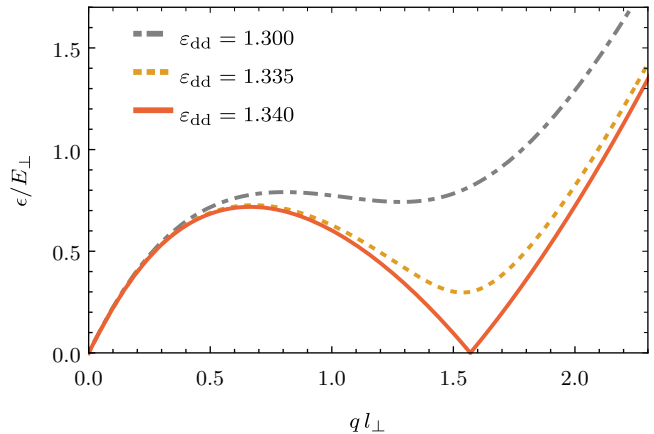


Figure 1. Excitation spectrum in the superfluid for different values of ε_{dd} for $\kappa_{\text{c}} = 11.931$ and $\lambda_{\text{c}} = 1/200$. By increasing ε_{dd} the spectrum develops a minimum, which eventually reaches zero energy at the critical point.

V. GROUND STATE IN THE SUPERSOLID REGIME

The roton instability indicates the formation of a new ground state with a density modulation with wavelength close to the corresponding roton momentum. Within our Bogoliubov approach, this is accounted for by the macroscopic occupation of not only the $q = 0$ mode, but also the modes with $q = lk_{\text{s}}$ with $l \in \mathbb{Z}$; the latter gives rise to a density modulation with momentum k_{s} and breaks the continuous translational symmetry resulting in a supersolid. In the following, we study first the ground state within this supersolid phase and in a next step its excitation spectrum. The mean-field ansatz takes the form

$$a_0 \rightarrow \sqrt{Ln_0} \quad \text{and} \quad a_{\pm lk_{\text{s}}} \rightarrow \frac{\Delta_l}{2} \sqrt{Ln_0} e^{\pm il\varphi},$$

with the order parameters Δ_l accounting for the solid structure. The bosonic field operator within mean-field theory is replaced by the condensate wave function

$$\Psi(z) \rightarrow \phi(z) \equiv \sqrt{n_0} \left(1 + \sum_{l=1}^{\infty} \Delta_l \cos[lk_{\text{s}}z + l\varphi] \right). \quad (6)$$

We also added a phase φ for the mean-field, which illustrates the possibility to freely shift the density wave in position. Different to our previous treatment, the zero momentum mode is not occupied by all particles and the total particle density is given by

$$n = \frac{1}{L} \int dz |\phi(z)|^2 = n_0 \left(1 + \sum_{l=1}^{\infty} \frac{\Delta_l^2}{2} \right). \quad (7)$$

Note that for only one order parameter, the ansatz in Eq. (6) reduces to the cosine-modulated ansatz used in [43]. Inserting the mean-field wave function into the effective Hamiltonian H , the energy depends on the order

parameters Δ_l as well as the wave vector k_s , i.e., $E(\Delta = (\Delta_1, \Delta_2, \dots, k_s))$, which is conveniently expressed by

$$E(\Delta) = - \int dz \phi^*(z) \frac{\hbar^2 \nabla^2}{2m} \phi(z) + N E_t(\sigma, \nu) + \frac{1}{2} \int dz dz' V(z - z') |\phi(z')|^2 |\phi(z)|^2 + \frac{2}{5} \gamma \int dz |\phi(z)|^5, \quad (8)$$

where $V(z)$ is the effective 1D interaction potential in real space. The energy has been evaluated analytically for up to four order parameters (see Appendix A), while including more order parameter will not drastically improve our ansatz (see below). Note that the energy also still depends on the transverse variational parameters σ and ν but not on the phase φ . Varying φ results in displacing the entire modulated state within the tube, and accounts for the broken continuous translation symmetry, which will give rise to an additional Goldstone mode [70]. Without loss of generality, we set $\varphi = 0$ in the following. The ground state is obtained by minimizing the energy $E(\Delta)$ with respect to Δ , σ and ν , under the constraint of a fixed particle number n in Eq. (7), resulting in the parameters Δ_{gs} . The superfluid state is then given by $\Delta_l = 0$, while the phase transition into the supersolid phase is characterized by a finite $\Delta_l \neq 0$. The chemical potential is determined by

$$\mu = \frac{1}{L} \frac{dE(\Delta_{\text{gs}})}{dn}.$$

Note, that Δ_{gs} also depends on the density n , but in analogy to the treatment in the superfluid phase we neglect the weak density dependence of the transverse degrees of freedom σ and ν .

Since the phase diagram of this model has been studied in [43] and an accurate phase diagram of the microscopic parameters would require to include the transverse degrees of freedom not only variationally, we focus on the parameters κ_c and λ_c that allow for a second-order phase transition and investigate the stability in the thermodynamic limit. In Fig. 2(a), we show the energy difference per particle, $\Delta E_l = (E(\Delta_{\text{gs}}) - E(0))/(E_{\perp} N)$, between the minimized energy in Eq. (8) when including l order parameter and the energy of the superfluid, $E(\Delta = 0)$. For $\varepsilon_{\text{dd}} < \varepsilon_{\text{dd},c}$ the energy difference vanishes and the superfluid is the ground state of the system. Increasing ε_{dd} beyond $\varepsilon_{\text{dd},c}$, we find a continuous phase transition into the supersolid phase. While a single order parameter very poorly describes the ground-state energy across the phase transition (black dashed line) the impact of more than two order parameter on the results is negligible within the studied parameter range. It shows that our ansatz converges fast with the number of order parameters. In Fig. 2(b) we show the four lowest order parameters Δ_l , which clearly exhibit a continuous behavior consistent with a second-order phase transition. In addition, the density modulation at the critical point

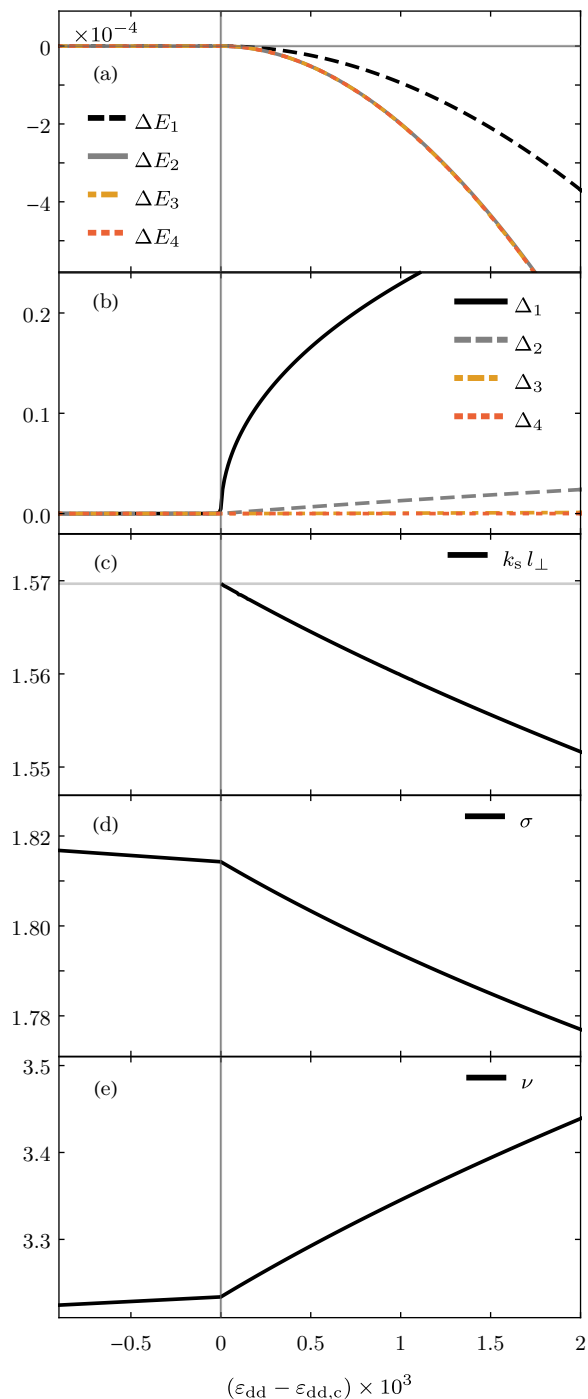


Figure 2. Ground state parameters across the superfluid to supersolid phase transition as a function of ε_{dd} for $\kappa_c = 11.931$ and $\lambda_c = 1/200$. (a) Energy difference per particle $\Delta E_l = (E(\Delta_{\text{gs}}) - E(0))/(E_{\perp} N)$ between the ground state of Eq.(8) and the superfluid when including $l = 1 \dots 4$ order parameters. (b) The four lowest order parameters used to obtain ΔE_4 as a function of ε_{dd} . (c) Wave vector k_s for the density modulation in the supersolid state. The gray horizontal line shows the roton momentum k_r . (d) Transverse width σ and (e) transverse anisotropy ν of the ground-state wave function.

appears at the position of the roton instability k_r , see Fig. 2(c), but k_s is slightly lowered for increasing ε_{dd} , i.e., the lattice spacing increases. This behavior can be understood as the side-by-side orientation of the dipoles pushes neighboring droplets further apart for increasing dipolar strength.

For the parameters κ_c and λ_c , a single order parameter does not describe the ground state accurately but predicts the correct type of phase transition, which is not generally true. For first-order transitions, including only a single order parameter can falsely predict a continuous transition, while including more order parameters clearly indicates a discontinuous transition, see Appendix B. Thus, we want to emphasize that a simple cosine-modulated ansatz for the supersolid can be very misleading.

VI. EXCITATIONS IN THE SUPERSOLID

Next, we study the excitation spectrum within the supersolid phase and generalize the procedure introduced for the superfluid. Since our results converge very fast with the number of order parameters, it is sufficient to include only two order parameters in the analysis. We again expand the field operator around the mean-field values $\Psi(z) = \phi(z) + \delta\psi(z)$ and derive the Hamiltonian up to second order in $\delta\psi(z)$, which leads to a quadratic Hamiltonian in the creation and annihilation operators $a_q^{(\dagger)}$. Due to the broken translational symmetry in the supersolid state, the excitations are only characterized by their quasi-momentum within the first Brillouin zone and couples states with a momentum difference by $\pm lk_s$. Therefore, the excitations exhibit a behavior similar to the well-known band structure in solids; however, as we are interested in the low-energy modes, we only analyze the lowest band. The Hamiltonian takes the form

$$H_B = \frac{1}{2} \sum_{q \in 1.\text{BZ}} : \begin{pmatrix} \mathbf{a}_+^\dagger \\ \mathbf{a}_- \end{pmatrix} \left[\begin{pmatrix} \chi & 0 \\ 0 & \chi \end{pmatrix} + \begin{pmatrix} \eta & \eta \\ \eta & \eta \end{pmatrix} \right] \begin{pmatrix} \mathbf{a}_+ \\ \mathbf{a}_-^\dagger \end{pmatrix} : \quad (9)$$

where

$$\mathbf{a}_\pm = \begin{pmatrix} a_{\pm q} \\ a_{\pm(q+k_s)} \\ a_{\pm(q-k_s)} \\ a_{\pm(q+2k_s)} \\ a_{\pm(q-2k_s)} \\ \vdots \end{pmatrix},$$

and the matrices χ and η depend on Δ_{gs} and the chemical potential μ . We obtain the excitation spectrum by diagonalizing the Hamiltonian in Eq.(9) via a Bogoliubov transformation $a_i = \sum_\alpha u_i^\alpha b_\alpha + v_i^\alpha b_{-\alpha}^\dagger$, where $i, \alpha \in \{q + lk_s, l \in \mathbb{Z}\}$. Finding the eigenmodes ϵ_s in the supersolid then reduces to finding the eigenvalues of $\chi^2 + 2\chi\eta$,

$$\det(\chi^2 + 2\chi\eta - \epsilon_s(q)^2 \mathbf{1}) = 0, \quad (10)$$

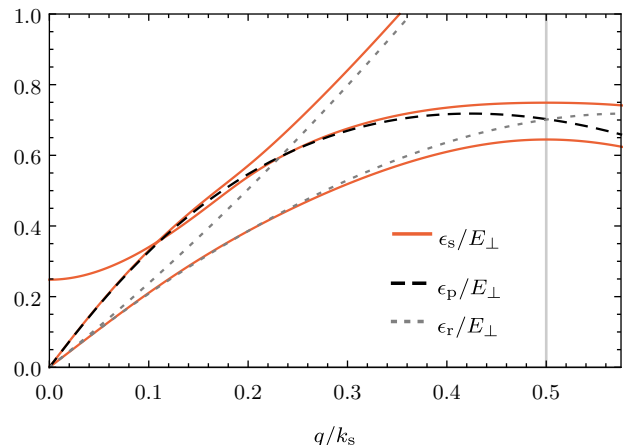


Figure 3. Excitation spectrum in the supersolid phase for $\varepsilon_{\text{dd}} = 1.3405$, $\lambda_c = 1/200$, and $\kappa_c = 11.931$. The red solid line shows the solution ϵ_s of Eq.(10) as a function of $q l_\perp$. The gray vertical lines indicate the first Brillouin zone. The black and gray dashed lines show the phonon and roton branches at the phase transition, respectively, and are used as a guide to the eye.

which generalizes Eq.(4) to systems where more than one mode is macroscopically occupied.

As shown in the previous discussion, the ground state close to the continuous phase transition is very accurately described by including two order parameters Δ_1 and Δ_2 , i.e., the modes with momenta $q = 0, \pm k_s, \pm 2k_s$ macroscopically occupied. In the derivation of the low-energy excitation spectrum, we work also with this accuracy. This allows us to restrict the size of the vectors \mathbf{a}_\pm to the 5 lowest momentum modes $q, q \pm k_s, q \pm 2k_s$ with q in the first Brillouin zone, and χ, η reduce to 5×5 matrices. We determine the expression for the matrices χ and η analytically (see Appendix C) and calculate the eigenvalues numerically.

In Fig.3 we show the excitation spectrum for $\varepsilon_{\text{dd}} = 1.3405$, close to the instability at $\varepsilon_{\text{dd},c} = 1.34$. The three red solid lines show the lowest eigenvalues $\epsilon_s(q l_\perp)/E_\perp$. The remaining two eigenvalues contribute to higher bands and are not shown. We have also added the roton modes ϵ_r (gray dotted lines) and the phonon mode ϵ_p (black dotted line) which were evaluated at the critical point; the gray vertical line indicates the first Brillouin zone. The excitation spectrum contains two gapless modes at $q = 0$, stemming from the broken $U(1)$ and translational symmetry in the supersolid, while the third mode shows a finite gap; the latter corresponds to the amplitude mode of the solid structure. It is important to point out that restricting the analysis to a single order parameter Δ_1 for the above parameters significantly alters the excitation spectrum. Especially the amplitude mode is strongly affected. Therefore, it is crucial to accurately describe the ground state within the supersolid phase and derive the excitation spectrum with high accuracy.

VII. CONCLUSION

We present a study of the excitation spectrum of a weakly interacting gas of dipolar bosons in a tight transverse harmonic confinement across the superfluid to supersolid phase transition. In a one-dimensional geometry, where the dipoles are aligned perpendicular to the tube, we introduce an effective Hamiltonian which includes beyond-mean-field effects in local-density approximation and make a variational ansatz for the transverse degrees of freedom. The transverse confinement in combination with the dipolar interaction leads to a roton spectrum in the superfluid. When the roton mode goes soft more than a single mode becomes macroscopically occupied and we adapt Bogoliubov theory by introducing an order parameter for each additional macroscopically occupied mode. This allows us to determine the ground-state energy and the excitation spectrum across the phase transition. For parameter comparable to cur-

rent Dysprosium experiments, we find that using one order parameter, which corresponds to a simple cosine-modulated ansatz for the ground-state wave function in the supersolid, is not enough to describe the system, neither in the continuous nor in the discontinuous transition regime. However, we show that our ansatz converges fast with the number of order parameters. The excitation spectrum in the supersolid regime close to a continuous transition shows no instabilities indicating the stability in the thermodynamic limit. In the low-energy regime we find two gapless modes in agreement with the two broken continuous symmetries as well as a gapped amplitude mode for the solid structure.

ACKNOWLEDGMENTS

We thank Tilman Pfau, Chris Bühler and Jens Hertkorn for fruitful discussions. This work is supported by the German Research Foundation (DFG) within FOR2247 under Bu2247/1-2.

-
- [1] L. Tanzi, E. Lucioni, F. Famà, J. Catani, A. Fioretti, C. Gabbanini, R. Bisset, L. Santos, and G. Modugno, Observation of a dipolar quantum gas with metastable supersolid properties, *Physical Review Letters* **122**, 130405 (2019).
 - [2] F. Böttcher, J.-N. Schmidt, M. Wenzel, J. Hertkorn, M. Guo, T. Langen, and T. Pfau, Transient supersolid properties in an array of dipolar quantum droplets, *Physical Review X* **9**, 10.1103/physrevx.9.011051 (2019).
 - [3] L. Chomaz, D. Petter, P. Ilzhöfer, G. Natale, A. Trautmann, C. Politi, G. Durastante, R. van Bijnen, A. Patscheider, M. Sohmen, M. Mark, and F. Ferlaino, Long-lived and transient supersolid behaviors in dipolar quantum gases, *Physical Review X* **9**, 021012 (2019).
 - [4] L. Santos, G. V. Shlyapnikov, and M. Lewenstein, Roton-maxon spectrum and stability of trapped dipolar bose-einstein condensates, *Physical Review Letters* **90**, 10.1103/physrevlett.90.250403 (2003).
 - [5] D. Petter, G. Natale, R. van Bijnen, A. Patscheider, M. Mark, L. Chomaz, and F. Ferlaino, Probing the roton excitation spectrum of a stable dipolar bose gas, *Physical Review Letters* **122**, 183401 (2019).
 - [6] I. Ferrier-Barbut, H. Kadau, M. Schmitt, M. Wenzel, and T. Pfau, Observation of quantum droplets in a strongly dipolar bose gas, *Phys. Rev. Lett.* **116**, 215301 (2016).
 - [7] D. S. Petrov, Quantum mechanical stabilization of a collapsing bose-bose mixture, *Phys. Rev. Lett.* **115**, 155302 (2015).
 - [8] F. Böttcher, J.-N. Schmidt, J. Hertkorn, K. S. H. Ng, S. D. Graham, M. Guo, T. Langen, and T. Pfau, New states of matter with fine-tuned interactions: quantum droplets and dipolar supersolids, *Reports on Progress in Physics* **84**, 012403 (2020).
 - [9] L. Chomaz, I. Ferrier-Barbut, F. Ferlaino, B. Laburthe-Tolra, B. L. Lev, and T. Pfau, Dipolar physics: A review of experiments with magnetic quantum gases (2022).
 - [10] A. J. Leggett, Can a solid be "superfluid"?, *Physical Review Letters* **25**, 1543 (1970).
 - [11] S. Balibar, The enigma of supersolidity, *Nature* **464**, 176 (2010).
 - [12] M. Boninsegni and N. V. Prokof'ev, Colloquium: Supersolids: What and where are they?, *Reviews of Modern Physics* **84**, 759 (2012).
 - [13] M. H. W. Chan, R. B. Hallock, and L. Reatto, Overview on solid 4He and the issue of supersolidity, *Journal of Low Temperature Physics* **172**, 317 (2013).
 - [14] H. Kadau, M. Schmitt, M. Wenzel, C. Wink, T. Maier, I. Ferrier-Barbut, and T. Pfau, Observing the rosenzweig instability of a quantum ferrofluid, *Nature* **530**, 194 (2016).
 - [15] I. Ferrier-Barbut, M. Schmitt, M. Wenzel, H. Kadau, and T. Pfau, Liquid quantum droplets of ultracold magnetic atoms, *Journal of Physics B: Atomic, Molecular and Optical Physics* **49**, 214004 (2016).
 - [16] L. Chomaz, S. Baier, D. Petter, M. J. Mark, F. Wächtler, L. Santos, and F. Ferlaino, Quantum-fluctuation-driven crossover from a dilute bose-einstein condensate to a macrodroplet in a dipolar quantum fluid, *Phys. Rev. X* **6**, 041039 (2016).
 - [17] M. Wenzel, F. Böttcher, T. Langen, I. Ferrier-Barbut, and T. Pfau, Striped states in a many-body system of tilted dipoles, *Phys. Rev. A* **96**, 053630 (2017).
 - [18] I. Ferrier-Barbut, M. Wenzel, F. Böttcher, T. Langen, M. Isoard, S. Stringari, and T. Pfau, Scissors mode of dipolar quantum droplets of dysprosium atoms, *Phys. Rev. Lett.* **120**, 160402 (2018).
 - [19] F. Wächtler and L. Santos, Ground-state properties and elementary excitations of quantum droplets in dipolar bose-einstein condensates, *Physical Review A* **94**, 043618 (2016).
 - [20] R. N. Bisset, R. M. Wilson, D. Baillie, and P. B. Blakie, Ground-state phase diagram of a dipolar condensate with

- quantum fluctuations, *Physical Review A* **94**, 033619 (2016).
- [21] A. Macia, J. Sánchez-Baena, J. Boronat, and F. Mazzanti, Droplets of trapped quantum dipolar bosons, *Physical Review Letters* **117**, 205301 (2016).
- [22] H. Saito, Path-integral monte carlo study on a droplet of a dipolar bose-einstein condensate stabilized by quantum fluctuation, *Journal of the Physical Society of Japan* **85**, 053001 (2016).
- [23] F. Cinti and M. Boninsegni, Classical and quantum filaments in the ground state of trapped dipolar bose gases, *Physical Review A* **96**, 013627 (2017).
- [24] M. Schmitt, M. Wenzel, F. Böttcher, I. Ferrier-Barbut, and T. Pfau, Self-bound droplets of a dilute magnetic quantum liquid, *Nature* **539**, 259 (2016).
- [25] F. Böttcher, M. Wenzel, J.-N. Schmidt, M. Guo, T. Langen, I. Ferrier-Barbut, T. Pfau, R. Bombín, J. Sánchez-Baena, J. Boronat, and F. Mazzanti, Dilute dipolar quantum droplets beyond the extended gross-pitaevskii equation, *Physical Review Research* **1**, 033088 (2019).
- [26] D. Baillie, R. M. Wilson, R. N. Bisset, and P. B. Blakie, Self-bound dipolar droplet: A localized matter wave in free space, *Physical Review A* **94**, 021602 (2016).
- [27] D. Baillie, R. M. Wilson, and P. B. Blakie, Collective excitations of self-bound droplets of a dipolar quantum fluid, *Phys. Rev. Lett.* **119**, 255302 (2017).
- [28] F. Cinti, A. Cappellaro, L. Salasnich, and T. Macrì, Superfluid filaments of dipolar bosons in free space, *Physical Review Letters* **119**, 215302 (2017).
- [29] M. Guo, F. Böttcher, J. Hertkorn, J.-N. Schmidt, M. Wenzel, H. P. Büchler, T. Langen, and T. Pfau, The low-energy goldstone mode in a trapped dipolar supersolid, *Nature* **574**, 386 (2019).
- [30] L. Tanzi, S. Rocuzzo, E. Lucioni, F. Famà, A. Fioretti, C. Gabbanini, G. Modugno, A. Recati, and S. Stringari, Supersolid symmetry breaking from compressional oscillations in a dipolar quantum gas, *Nature* **574**, 382 (2019).
- [31] G. Natale, R. M. W. van Bijnen, A. Patscheider, D. Petter, M. J. Mark, L. Chomaz, and F. Ferlaino, Excitation spectrum of a trapped dipolar supersolid and its experimental evidence, *Phys. Rev. Lett.* **123**, 050402 (2019).
- [32] L. Tanzi, J. G. Maloberti, G. Biagioni, A. Fioretti, C. Gabbanini, and G. Modugno, Evidence of superfluidity in a dipolar supersolid from nonclassical rotational inertia, *Science* **371**, 1162 (2021).
- [33] M. Sohmen, C. Politi, L. Klaus, L. Chomaz, M. J. Mark, M. A. Norcia, and F. Ferlaino, Birth, life, and death of a dipolar supersolid, *Physical Review Letters* **126**, 233401 (2021).
- [34] D. Petter, A. Patscheider, G. Natale, M. J. Mark, M. A. Baranov, R. van Bijnen, S. M. Rocuzzo, A. Recati, B. Blakie, D. Baillie, L. Chomaz, and F. Ferlaino, Bragg scattering of an ultracold dipolar gas across the phase transition from bose-einstein condensate to supersolid in the free-particle regime, *Physical Review A* **104**, 1011302 (2021).
- [35] G. Biagioni, N. Antolini, A. Alaña, M. Modugno, A. Fioretti, C. Gabbanini, L. Tanzi, and G. Modugno, Dimensional crossover in the superfluid-supersolid quantum phase transition, *Physical Review X* **12**, 021019 (2022).
- [36] T. Bland, E. Poli, C. Politi, L. Klaus, M. Norcia, F. Ferlaino, L. Santos, and R. Bisset, Two-dimensional supersolid formation in dipolar condensates, *Physical Review Letters* **128**, 195302 (2022).
- [37] M. A. Norcia, E. Poli, C. Politi, L. Klaus, T. Bland, M. J. Mark, L. Santos, R. N. Bisset, and F. Ferlaino, Can angular oscillations probe superfluidity in dipolar supersolids?, *Physical Review Letters* **129**, 040403 (2022).
- [38] S. M. Rocuzzo and F. Ancilotto, Supersolid behavior of a dipolar bose-einstein condensate confined in a tube, *Physical Review A* **99**, 041601 (2019).
- [39] J. Hertkorn, F. Böttcher, M. Guo, J. Schmidt, T. Langen, H. Büchler, and T. Pfau, Fate of the amplitude mode in a trapped dipolar supersolid, *Physical Review Letters* **123**, 10.1103/physrevlett.123.193002 (2019).
- [40] Y.-C. Zhang, F. Maucher, and T. Pohl, Supersolidity around a critical point in dipolar bose-einstein condensates, *Physical Review Letters* **123**, 015301 (2019).
- [41] S. Rocuzzo, A. Gallemí, A. Recati, and S. Stringari, Rotating a supersolid dipolar gas, *Physical Review Letters* **124**, 045702 (2020).
- [42] A. Gallemí, S. M. Rocuzzo, S. Stringari, and A. Recati, Quantized vortices in dipolar supersolid bose-einstein condensed gases, *Physical Review A* **102**, 023322 (2020).
- [43] P. B. Blakie, D. Baillie, L. Chomaz, and F. Ferlaino, Supersolidity in an elongated dipolar condensate, *Physical Review Research* **2**, 043318 (2020).
- [44] Y.-C. Zhang, T. Pohl, and F. Maucher, Phases of supersolids in confined dipolar bose-einstein condensates, *Physical Review A* **104**, 013310 (2021).
- [45] F. Ancilotto, M. Barranco, M. Pi, and L. Reatto, Vortex properties in the extended supersolid phase of dipolar bose-einstein condensates, *Physical Review A* **103**, 033314 (2021).
- [46] J. Hertkorn, J.-N. Schmidt, M. Guo, F. Böttcher, K. S. H. Ng, S. D. Graham, P. Uerlings, T. Langen, M. Zwierlein, and T. Pfau, Pattern formation in quantum ferrofluids: From supersolids to superglasses, *Physical Review Research* **3**, 033125 (2021).
- [47] J. Hertkorn, J.-N. Schmidt, M. Guo, F. Böttcher, K. Ng, S. Graham, P. Uerlings, H. Büchler, T. Langen, M. Zwierlein, and T. Pfau, Supersolidity in two-dimensional trapped dipolar droplet arrays, *Physical Review Letters* **127**, 155301 (2021).
- [48] E. Poli, T. Bland, C. Politi, L. Klaus, M. A. Norcia, F. Ferlaino, R. N. Bisset, and L. Santos, Maintaining supersolidity in one and two dimensions, *Physical Review A* **104**, 063307 (2021).
- [49] S. M. Rocuzzo, A. Recati, and S. Stringari, Moment of inertia and dynamical rotational response of a supersolid dipolar gas, *Physical Review A* **105**, 023316 (2022).
- [50] J. Sánchez-Baena, C. Politi, F. Maucher, F. Ferlaino, and T. Pohl, Heating a quantum dipolar fluid into a solid (2022).
- [51] C. Bühler, T. Ilg, and H. P. Büchler, Quantum fluctuations in one-dimensional supersolids, (2022), submitted for publication.
- [52] M. Šindik, A. Recati, S. M. Rocuzzo, L. Santos, and S. Stringari, Creation and robustness of quantized vortices in a dipolar supersolid when crossing the superfluid-to-supersolid transition (2022).
- [53] R. Bombin, J. Boronat, and F. Mazzanti, Dipolar bose supersolid stripes, *Physical Review Letters* **119**, 250402 (2017).
- [54] R. Bombín, F. Mazzanti, and J. Boronat, Berezinskii-kosterlitz-thouless transition in two-dimensional dipolar stripes, *Physical Review A* **100**, 063614 (2019).

- [55] C. R. Cabrera, L. Tanzi, J. Sanz, B. Naylor, P. Thomas, P. Cheiney, and L. Tarruell, Quantum liquid droplets in a mixture of bose-einstein condensates, *Science* **359**, 301 (2017).
- [56] T. Ilg, J. Kumlin, L. Santos, D. S. Petrov, and H. P. Büchler, Dimensional crossover for the beyond-mean-field correction in bose gases, *Phys. Rev. A* **98**, 051604 (2018).
- [57] P. B. Blakie, D. Baillie, and S. Pal, Variational theory for the ground state and collective excitations of an elongated dipolar condensate, *Communications in Theoretical Physics* **72**, 085501 (2020).
- [58] M. Olshanii, Atomic scattering in the presence of an external confinement and a gas of impenetrable bosons, *Phys. Rev. Lett.* **81**, 938 (1998).
- [59] A. R. P. Lima and A. Pelster, Quantum fluctuations in dipolar bose gases, *Physical Review A* **84**, 041604 (2011).
- [60] A. R. P. Lima and A. Pelster, Beyond mean-field low-lying excitations of dipolar bose gases, *Phys. Rev. A* **86**, 063609 (2012).
- [61] T. D. Lee and C. N. Yang, Many-body problem in quantum mechanics and quantum statistical mechanics, *Phys. Rev.* **105**, 1119 (1957).
- [62] T. D. Lee, K. Huang, and C. N. Yang, Eigenvalues and eigenfunctions of a bose system of hard spheres and its low-temperature properties, *Phys. Rev.* **106**, 1135 (1957).
- [63] N. Bogoliubov, On the theory of superfluidity, *J. Phys* **11**, 23 (1947).
- [64] E. H. Lieb and W. Liniger, Exact analysis of an interacting bose gas. i. the general solution and the ground state, *Phys. Rev.* **130**, 1605 (1963).
- [65] E. H. Lieb, Exact analysis of an interacting bose gas. ii. the excitation spectrum, *Phys. Rev.* **130**, 1616 (1963).
- [66] F. D. M. Haldane, Effective harmonic-fluid approach to low-energy properties of one-dimensional quantum fluids, *Physical Review Letters* **47**, 1840 (1981).
- [67] D. S. Petrov, G. V. Shlyapnikov, and J. T. M. Walraven, Regimes of quantum degeneracy in trapped 1d gases, *Phys. Rev. Lett.* **85**, 3745 (2000).
- [68] N. M. Hugenholtz and D. Pines, Ground-state energy and excitation spectrum of a system of interacting bosons, *Phys. Rev.* **116**, 489 (1959).
- [69] T. Lahaye, C. Menotti, L. Santos, M. Lewenstein, and T. Pfau, The physics of dipolar bosonic quantum gases, *Reports on Progress in Physics* **72**, 126401 (2009).
- [70] H. Nielsen and S. Chadha, On how to count goldstone bosons, *Nuclear Physics B* **105**, 445 (1976).

Appendix A: Ground-state energy

We obtain the energy in the supersolid phase as a function of Δ by inserting the mean-field ansatz Eq. (6) into the energy functional Eq. (8). For four order parameters, we evaluate the integrals analytically and obtain $E = NE_t + E_{\text{kin}} + E_{\text{int}} + E_{\text{LHY}}$, where

$$\begin{aligned} \frac{E_{\text{kin}}}{N} &= E_{\perp} \frac{(k_s l_{\perp})^2}{4} \frac{\Delta_1^2 + 4\Delta_2^2 + 9\Delta_3^2 + 16\Delta_4^2}{1 + \frac{\Delta_1^2}{2} + \frac{\Delta_2^2}{2} + \frac{\Delta_3^2}{2} + \frac{\Delta_4^2}{2}}, \\ \frac{E_{\text{int}}}{N} &= \left[\frac{(2 + \Delta_1^2 + \Delta_2^2 + \Delta_3^2 + \Delta_4^2)^2}{2} nV(0) + (\Delta_1(2 + \Delta_2) + \Delta_3(\Delta_2 + \Delta_4))^2 nV(k_s) \right. \\ &\quad + \frac{(\Delta_1^2 + 2\Delta_1\Delta_3 + 2\Delta_2(2 + \Delta_4))^2}{4} nV(2k_s) + (2\Delta_3 + \Delta_1(\Delta_2 + \Delta_4))^2 nV(3k_s) \\ &\quad + \frac{(\Delta_2^2 + 2\Delta_1\Delta_3 + 4\Delta_4)^2}{4} nV(4k_s) + (\Delta_2\Delta_3 + \Delta_1\Delta_4)^2 nV(5k_s) \\ &\quad \left. + \frac{(\Delta_3^2 + 2\Delta_2\Delta_4)^2}{4} nV(6k_s) + \Delta_3^2\Delta_4^2 nV(7k_s) + \frac{\Delta_4^4}{4} nV(8k_s) \right] / (2 + \Delta_1^2 + \Delta_2^2 + \Delta_3^2 + \Delta_4^2)^2. \end{aligned}$$

Close to the phase transition $1 + \sum_{l=1}^4 \Delta_l \cos(lx) > 0 \forall x$ and the absolute value in Eq. (8) can be ignored which yields

$$\begin{aligned} \frac{E_{\text{LHY}}}{N} &= \gamma n^{3/2} \left[\frac{2}{5} + \frac{1}{8} \left(\Delta_1^4 (6 + 4\Delta_2 + \Delta_4) + 4\Delta_1^3 \Delta_3 (2 + 3\Delta_2 + 3\Delta_4) \right. \right. \\ &\quad + 2\Delta_1^2 (8 + 3\Delta_2^3 + 12\Delta_4^2 + 6\Delta_2^2 (2 + \Delta_4) + 3\Delta_3^2 (4 + \Delta_4) + 6\Delta_2 (2 + \Delta_3^2 + \Delta_4 (2 + \Delta_4))) \\ &\quad + 12\Delta_1 \Delta_3 (\Delta_2^3 + 2\Delta_2^2 (1 + \Delta_4) + \Delta_4 (4 + \Delta_3^2 + \Delta_4^2) + \Delta_2 (4 + \Delta_3^2 + 2\Delta_4 (2 + \Delta_4))) \\ &\quad + 2(\Delta_2^3 \Delta_3^2 + 3\Delta_3^4 + 8\Delta_4^2 + 3\Delta_4^4 + 3\Delta_2 \Delta_3^2 \Delta_4 (4 + \Delta_4) + \Delta_4^2 (3 + 2\Delta_4) + 4\Delta_2^2 (2 + 3\Delta_4^2)) \\ &\quad \left. \left. + 2(\Delta_2^2 (8 + 6\Delta_3^2 (2 + \Delta_4) + 3\Delta_4 (2 + \Delta_4)^2)) \right) \right] / \left(1 + \frac{\Delta_1^2}{2} + \frac{\Delta_2^2}{2} + \frac{\Delta_3^2}{2} + \frac{\Delta_4^2}{2} \right)^{5/2}. \end{aligned}$$

The ground state is then obtained by minimizing the energy with respect to $\Delta_1, \dots, \Delta_4, k_s, \sigma$ and ν .

Appendix B: First-order Transition

In addition to the continuous transition discussed in the main text, we briefly want to comment on first-order transitions within our approach. By fixing the critical values to $\kappa_c = 9.982$ and $\lambda_c = 1/220$, the roton instability again appears at $\varepsilon_{\text{dd,c}} = 1.34$, however, since κ_c and λ_c are smaller compared to the values chosen in the main text ($\kappa_c = 11.931$, $\lambda_c = 1/200$) the term $\lambda \kappa^{3/2} \sim H_{\text{LHY}}/N$ is too small and the transition is of first order. This becomes apparent in Fig.4 where we show the system parameter across the phase transition. For Fig. 4(a)-(e), we only include a single order parameter in our approach, which corresponds to a simple cosine-modulated ansatz. The energy difference per particle ΔE_1 in Fig. 4(a), the order parameter Δ_1 in Fig 4(b), the modulation k_s in Fig. 4(c) as well as the transverse width σ in Fig. 4(d) and the transverse anisotropy ν in Fig. 4(e) all indicate a second-order phase transition, analogously to the parameter regime in the main text. Including more order parameter, the discussion changes drastically. By including more order parameters we find that the ground-state energy can be lowered even for $\varepsilon_{\text{dd}} < \varepsilon_{\text{dd,c}}$ (see Fig. 4(f)) indicating a first-order phase transition. For Fig. 4(g)-(j) we show the system parameter when including four order parameter. In Fig. 4(g), the lowest order parameters Δ_l show a jump to a finite value at $\varepsilon_{\text{dd}} \approx 1.3395$. This discontinuous behavior also shows in the width in Fig. 2(i) and anisotropy in Fig. 2(j) of the ground-state wave function. The modulation of the ground state never coincides with the roton momentum, see Fig. 2(h). The previous discussion shows that a simple cosine-modulated ansatz can be very misleading for characterizing the properties of the ground state.

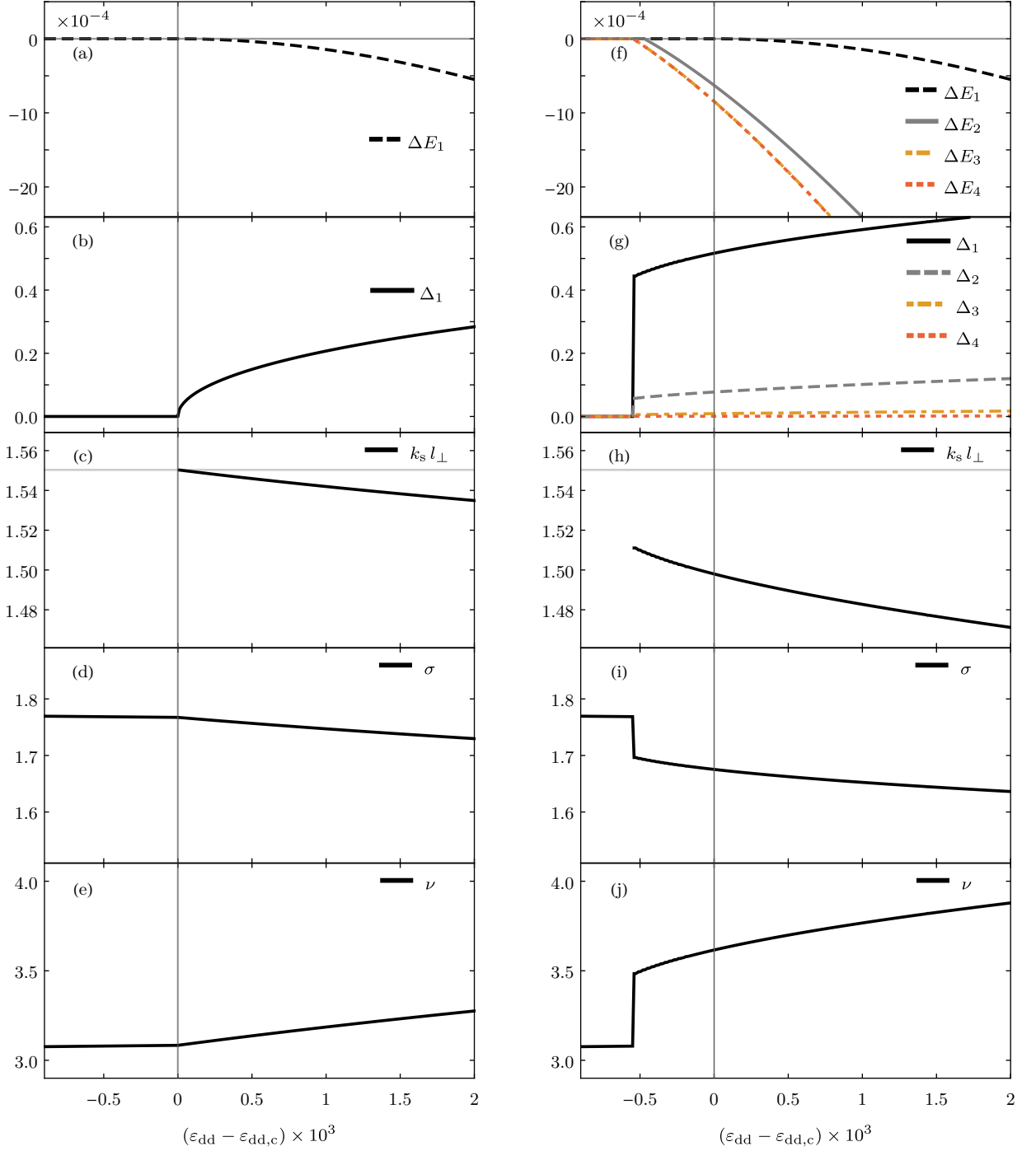


Figure 4. Ground state parameters across the superfluid to supersolid phase transition as a function of ϵ_{dd} for $\kappa_c = 9.982$ and $\lambda_c = 1/220$. For (a)-(e) we only include a single order parameter. (a) Energy difference per particle ΔE_1 . (b) Order parameter used to obtain ΔE_1 as a function of ϵ_{dd} . (c) Wave vector k_s for the density modulation of the supersolid state. (d) Transverse width σ and (e) transverse anisotropy ν of the ground-state wave function. (f) Energy difference per particle ΔE_l when including $l = 1 \dots 4$ order parameter. For (g)-(j) we include four order parameter to obtain the system parameters analog to (b)-(e).

Appendix C: Excitations

We calculate the matrices χ and η by including two order parameters and expanding the Hamiltonian Eq. 2 up to quadratic order in the creation and annihilation operators. We obtain

$$\chi = \mathbf{x} + \frac{1}{2} \frac{\gamma n^{3/2}}{(1 + \frac{\Delta_1^2}{2} + \frac{\Delta_2^2}{2})^{3/2}} \mathbf{\Lambda} \quad \text{and} \quad \eta = \frac{\mathbf{h}}{1 + \frac{\Delta_1^2}{2} + \frac{\Delta_2^2}{2}} + \frac{3}{4} \frac{\gamma n^{3/2}}{(1 + \frac{\Delta_1^2}{2} + \frac{\Delta_2^2}{2})^{3/2}} \mathbf{\Lambda}$$

where \mathbf{x} , \mathbf{h} and $\mathbf{\Lambda}$ are symmetric 5×5 matrices with entries

$$\begin{aligned} x_{11} &= \epsilon_0(q) - \mu + E_t + nV(0) \\ x_{22} &= \epsilon_0(q + k_s) - \mu + E_t + nV(0) \\ x_{33} &= \epsilon_0(q - k_s) - \mu + E_t + nV(0) \\ x_{44} &= \epsilon_0(q + 2k_s) - \mu + E_t + nV(0) \\ x_{55} &= \epsilon_0(q - 2k_s) - \mu + E_t + nV(0) \\ x_{12} = x_{13} = x_{24} = x_{35} &= \frac{\Delta_1 (\frac{\Delta_2}{2} + 1) nV(k_s)}{1 + \frac{\Delta_1^2}{2} + \frac{\Delta_2^2}{2}} \\ x_{14} = x_{15} = x_{23} &= \frac{(\frac{\Delta_1^2}{4} + \Delta_2) nV(2k_s)}{1 + \frac{\Delta_1^2}{2} + \frac{\Delta_2^2}{2}} \\ x_{25} = x_{34} &= \frac{\Delta_1 \Delta_2 nV(3k_s)}{2(1 + \frac{\Delta_1^2}{2} + \frac{\Delta_2^2}{2})} \\ x_{45} &= \frac{\Delta_2^2 nV(4k_s)}{4(1 + \frac{\Delta_1^2}{2} + \frac{\Delta_2^2}{2})} \\ \Lambda_{i,i} &= 2 \left(\frac{3}{4} \Delta_2 \Delta_1^2 + \frac{3\Delta_1^2}{2} + \frac{3\Delta_2^2}{2} + 1 \right) \\ \Lambda_{12} = \Lambda_{13} = \Lambda_{24} = \Lambda_{35} &= \frac{3\Delta_1^3}{4} + \frac{3}{2} \Delta_2^2 \Delta_1 + 3\Delta_2 \Delta_1 + 3\Delta_1 \\ \Lambda_{14} = \Lambda_{15} = \Lambda_{23} &= \frac{3\Delta_2^3}{4} + \frac{3}{2} \Delta_1^2 \Delta_2 + 3\Delta_2 + \frac{3\Delta_1^2}{2} \\ \Lambda_{25} = \Lambda_{34} &= \frac{\Delta_1^3}{4} + \frac{3}{4} \Delta_2^2 \Delta_1 + 3\Delta_2 \Delta_1 \\ \Lambda_{45} &= \frac{3}{4} \Delta_2 \Delta_1^2 + \frac{3\Delta_2^2}{2} \\ h_{11} &= \frac{\Delta_1^2}{4} [nV(q - k_s) + nV(k_s + q)] + \frac{\Delta_2^2}{4} [nV(q - 2k_s) + nV(2k_s + q)] + nV(q) \\ h_{22} &= \frac{\Delta_1^2}{4} [nV(2k_s + q) + nV(q)] + \frac{\Delta_2^2}{4} [nV(q - k_s) + nV(3k_s + q)] + nV(k_s + q) \\ h_{33} &= \frac{\Delta_1^2}{4} [nV(q - 2k_s) + nV(q)] + \frac{\Delta_2^2}{4} [nV(q - 3k_s) + nV(k_s + q)] + nV(q - k_s) \\ h_{44} &= \frac{\Delta_1^2}{4} [nV(k_s + q) + nV(3k_s + q)] + \frac{\Delta_2^2}{4} [nV(4k_s + q) + nV(q)] + nV(2k_s + q) \\ h_{55} &= \frac{\Delta_1^2}{4} [nV(q - 3k_s) + nV(q - k_s)] + \frac{\Delta_2^2}{4} [nV(q - 4k_s) + nV(q)] + nV(q - 2k_s) \\ h_{12} &= \frac{\Delta_1}{2} [nV(k_s + q) + nV(q)] + \frac{\Delta_1 \Delta_2}{4} [nV(q - k_s) + nV(2k_s + q)] \\ h_{13} &= \frac{\Delta_1}{2} [nV(q - k_s) + nV(q)] + \frac{\Delta_1 \Delta_2}{4} [nV(q - 2k_s) + nV(k_s + q)] \\ h_{14} &= \frac{\Delta_1^2}{4} nV(k_s + q) + \frac{\Delta_2}{2} [nV(2k_s + q) + nV(q)] \end{aligned}$$

$$\begin{aligned}
h_{15} &= \frac{\Delta_1^2}{4} nV(q - k_s) + \frac{\Delta_2}{2} [nV(q - 2k_s) + nV(q)] \\
h_{23} &= \frac{\Delta_2}{2} [nV(q - k_s) + nV(k_s + q)] + \frac{\Delta_1^2}{4} nV(q) \\
h_{24} &= \frac{\Delta_1}{2} [nV(k_s + q) + nV(2k_s + q)] + \frac{\Delta_1 \Delta_2}{4} [nV(3k_s + q) + nV(q)] \\
h_{25} &= \frac{\Delta_1 \Delta_2}{4} [nV(q - k_s) + nV(q)] \\
h_{34} &= \frac{\Delta_1 \Delta_2}{4} [nV(k_s + q) + nV(q)] \\
h_{35} &= \frac{\Delta_1 \Delta_2}{4} [nV(q - 3k_s) + nV(q)] + \frac{\Delta_1}{2} [nV(q - 2k_s) + nV(q - k_s)] \\
h_{45} &= \frac{\Delta_2^2}{4} nV(q).
\end{aligned}$$